Bezafibrate improves insulin sensitivity and metabolic flexibility in STZ-treated diabetic mice

Running title: Bezafibrate improves insulin sensitivity in STZ mice

Andras Franko[1,2,3], Peter Huypens[1,3], Susanne Neschen[1,3,4,20], Martin Irmler[1], Jan Rozman[1,3,4], Birgit Rathkolb[1,4,5], Frauke Neff[1,6], Cornelia Prehn[7], Guillaume Dubois[1], Martina Baumann[1], Rebecca Massinger[1], Daniel Gradinger[1,3], Gerhard K. H. Przemeck[1,3], Birgit Repp[8], Michaela Aichler[9], Annette Feuchtinger[9], Philipp Schommers[10,11], Oliver Stöhr[12], Carmen Sanchez-Lasheras[13], Jerzy Adamski[3,7,14], Andreas Peter[2,3,15], Holger Prokisch[8], Johannes Beckers[1,3,16], Axel K. Walch[9], Helmut Fuchs[1,3,4], Eckhard Wolf[5], Markus Schubert[12,17], Rudolf J. Wiesner[10,18,19], Martin Hrabě de Angelis[1,3,4,16]

1 Institute of Experimental Genetics, Helmholtz Zentrum München, Neuherberg

2 Department of Internal Medicine, Division of Endocrinology, Diabetology, Angiology, Nephrology and Clinical Chemistry, University Hospital Tübingen, Tübingen

3 German Center for Diabetes Research (DZD e.V.), Neuherberg

4 German Mouse Clinic, Helmholtz Zentrum München, Neuherberg

5 Institute of Molecular Animal Breeding and Biotechnology, Ludwig Maximilians-Universität-München, München

6 Institute of Pathology, Helmholtz Zentrum München, Neuherberg

7 Genome Analysis Center, Institute of Experimental Genetics, Helmholtz Zentrum München, Neuherberg

8 Institute of Human Genetics, Helmholtz Zentrum München, Neuherberg

9 Research Unit Analytical Pathology, Helmholtz Zentrum München, Neuherberg

10 Institute of Vegetative Physiology, University of Köln, Cologne

11 Department I of Internal Medicine, University Hospital Cologne, Cologne

Diabetes Publish Ahead of Print, published online June 9, 2016

12 Center for Endocrinology, Diabetes and Preventive Medicine, University of Köln, Cologne

13 Institute of Genetics, University of Köln, Cologne

14 Lehrstuhl für Experimentelle Genetik, Technische Universität München, Freising-Weihenstephan

15 Institute for Diabetes Research and Metabolic Diseases of the Helmholtz Centre Munich at the University of Tübingen, Tübingen

16 Center of Life and Food Sciences Weihenstephan, Technische Universität München, Freising

17 Internal Medicine, SCIVIAS Hospital St. Josef, Rüdesheim am Rhein

18 Center for Molecular Medicine Cologne (CMMC), University of Köln, Cologne,

19 Cologne Excellence Cluster on Cellular Stress Responses in Ageing-associated Diseases (CECAD), University of Köln, Cologne, Germany

20 Current address: Sanofi-Aventis Deutschland GmbH, R&D Diabetes Research & Translational Medicine, Industriepark Hoechst, 65926 Frankfurt am Main, Germany.

Corresponding author:

Dr. Martin Hrabě de Angelis

Helmholtz Zentrum München, German Research Center for Environmental Health (GmbH),

Ingolstädter Landstraße 1, 85764 Neuherberg, Germany

Phone: + 49 89 3187 3502

Fax: + 49 89 3187 3500

Email: hrabe@helmholtz-muenchen.de

Word count: 4205

Number of figures: 5

Number of tables: 2

Abstract

Bezafibrate (BEZ), a pan activator of peroxisome proliferator-activated receptors (PPARs), has been generally used to treat hyperlipidemia for decades. Clinical trials with type 2 diabetes patients indicated that BEZ also has beneficial effects on glucose metabolism, although the underlying mechanisms of these effects remain elusive. Even less is known about a potential role for BEZ in treating type 1 diabetes. Here we show that BEZ markedly improves hyperglycemia and glucose and insulin tolerance in streptozotocin (STZ)-treated mice, an insulin-deficient mouse model of type 1 diabetes. BEZ treatment of STZ mice significantly suppressed the hepatic expression of genes that are annotated in inflammatory processes, whereas the expression of PPAR and insulin target gene transcripts was increased. Furthermore, BEZ-treated mice also exhibited improved metabolic flexibility as well as an enhanced mitochondrial mass and function in the liver. Finally, we show that the number of pancreatic islets and the area of insulin positive cells tended to be higher in BEZ-treated mice. Our data suggest that BEZ may improve impaired glucose metabolism by augmenting hepatic mitochondrial performance, suppressing hepatic inflammatory pathways, and improving insulin sensitivity and metabolic flexibility. Thus, BEZ treatment might also be useful for patients with impaired glucose tolerance or diabetes.

Abbreviations

Bezafibrate (BEZ), blood glucose (BG), control non-treated mice (Con), electron microscopy (EM), non-esterified fatty acid (NEFA), peroxisomal proliferator activated receptor (PPAR), quantitative nuclear magnetic resonance (qNMR), quantitative sensitivity check index (QUICKI), respiratory exchange ratios (RER), standard diet (SD), streptozotocin (STZ), triglyceride (TG)

Keywords

insulin-deficient type 1 diabetes, insulin resistance, mitochondria, PPAR, STZ

Introduction

Bezafibrate (BEZ) has been used to treat patients with high lipid levels (1-3). The beneficial effect of BEZ on lipid metabolism is attributed to the activation of the transcription factor family of peroxisomal proliferator activated receptors (PPARs, PPARα, PPARβ/δ, PPARγ) (4). BEZ treatment is also associated with a lower prevalence of type 2 diabetes in high-risk populations (5), and decreased blood glucose levels in patients with established type 2 diabetes (6). Since lipid and glucose metabolism are closely linked (7), the decreased prevalence of type 2 diabetes in BEZ-treated patients is not completely unexpected, although the underlying molecular mechanisms of BEZ action remain unclear.

In addition to its beneficial effects on lipid and glucose metabolism, BEZ is also reported to directly improve skeletal muscle mitochondrial function in patients and mice with mitochondrial dysfunction (8, 9). We previously demonstrated that mitochondrial capacity is impaired in skeletal muscle of STZ mice (10) and considering that mitochondria play a pivotal role in both glucose and lipid metabolism (7), we postulated that BEZ could ameliorate impaired glucose/lipid metabolism by stimulating mitochondrial performance in metabolic organs.

Research Design and Methods

Materials

All chemicals were purchased from Sigma-Aldrich (Germany) unless otherwise stated.

Animal studies

Male C57BL/6N mice were purchased from Charles River. Twelve week-old mice were injected with 60 mg/kg STZ on five consecutive days (10). In an initial experiment, aiming at studying muscle, BEZ treatment started 8 weeks after STZ injection (Suppl. Fig. 1A-C). For all other experiments, BEZ treatment began 2 weeks after STZ injection. Mice received a standard diet (SD) (R/M-H, Ssniff, Germany), which was supplemented with 0.25% or 0.5%

(w/w) BEZ (B7273, Sigma-Aldrich) for the BEZ groups. Animals were killed by isoflurane overdose and dissected tissues were immediately frozen in liquid nitrogen, unless otherwise stated. All mouse studies were approved by local government authorities and performed according to GV-SOLAS (Society for Laboratory Animal Science) in accordance with the German Animal Welfare Act.

Plasma triglyceride (TG), non-esterified fatty acid (NEFA), creatinine, creatine kinase, urea and C-reactive peptide (CRP) levels were quantified by routine clinical chemistry using an AU480 analyzer (Beckman Coulter, Germany) (11). Blood glucose and hemoglobin A1c levels were measured in tail blood samples using a glucometer (Contour, Bayer, Germany) and the Clover A1c Self system (Obelis, Belgium). Insulin levels were determined by ELISA (Mercodia, Sweden) or a Bio-Plex Pro mouse diabetes immunoassay (Bio-Rad, Germany). Intraperitoneal glucose and insulin tolerance tests were performed with 1 g/kg glucose or 0.5 U/kg insulin. Quantitative insulin sensitivity check index (QUICKI) values were calculated as: 1/(log(fasting insulin µU/mL)+log(fasting glucose mg/dL)). Body composition and energy balance were determined by qNMR (MiniSpec LF60, Bruker Optics, Germany). Indirect calorimetry (PhenoMaster System, TSE Systems, Germany) was conducted as described previously (11). A linear regression model including body weight as a co-variate was used to adjust for body weight-dependent differences in energy metabolism parameters (TIBCO Spotfire S+ 8.1 for Windows).

Human cells

Patients with a possible complex I deficiency according to the clinical phenotype were analyzed by muscle biopsy. Those who showed deficient complex I-driven respiration in skeletal muscle and mutations in mitochondrial genes revealed by gDNA sequencing were selected for the study. Skin samples were taken for fibroblast isolation (12-14). The NHDF-neo cell line (Lonza, Germany) was used as a healthy control. Cells were grown under

standard conditions (DMEM, 4.5 g/l glucose supplemented with 10% FBS) and treated with 400 μM BEZ for 72 hours.

Oxygen consumption measurements

Mitochondrial respiration was determined in *soleus* muscles as described earlier (10). Mitochondrial respiration was determined in digitonin-permeabilized fibroblasts using high-resolution respirometry (Oroboros Oxygraph-2k, Austria). In brief, we measured Complex I respiration using glutamate/malate (10 mM/5 mM), ADP (1 mM), rotenone (0.5 μM), followed by measurement of Complex II respiration using succinate (10 mM), antimycin A (2.5 μM) followed by Complex IV respiration after addition of TMPD (tetramethylphenylendiamin) and ascorbate (2 mM/0.5 mM). Respiration rates were normalized to cell number and the lowest values for control fibroblasts were set as 100%.

Mouse mitochondria were freshly isolated from 100-150 mg liver samples with a gentleMACS Dissociator and the Mitochondria Isolation Kit (Miltenyi Biotec, Germany). Oxygen consumption was determined using an XF Extracellular Flux Analyzer (XF96, Seahorse Bioscience, USA) as recently described (15). Mitochondrial protein (2 μg) was added to individual wells of 96-well plates for the following protocols: i) electron flow assay, 10 mM pyruvate, 2 mM malate were given as substrates, and 2 μM rotenone (Port A), 10 mM succinate (Port B), 4 μM antimycin A (Port C), 100 μM TMPD and 10 mM ascorbate (Port D) were used; ii) coupling assay, 10 mM succinate was given as a substrate in combination with 2 μM rotenone, and 4 mM ADP (Port A), 2 μM oligomycin (Port B), 4 μM FCCP (Port C) and 4 μM antimycin A (Port D) were applied. All values represent final concentrations in the assay buffer (MAS).

Real-time PCR

Tibialis cranialis muscles were homogenized in liquid nitrogen, total RNA was prepared and expression of mitochondrial genes was studied by real-time PCR as described (10). Mouse

livers were pulverized in liquid nitrogen and total RNA was prepared using an miRNeasy Mini kit (Qiagen, Germany). cDNA was prepared by reverse transcription (Invitrogen, Germany) and real-time PCR assays were carried out with a LC480 Light Cycler (Roche, Germany) using the applied primer sequences listed in Supplementary Table 1.

Microarrays

Amplification of total RNA and array processing (mouse Affymetrix Gene 1.0 ST) were done as previously described (16). Array data were submitted to the NCBI GEO database (GSE39752, GSE79008). Statistical analysis was performed in MeV (MultiExperiment Viewer, 4.9.0) using the Significance Analysis of Microarrays (SAM) algorithm with 1,000 permutations and a local False Discovery Rate (FDR)<10%. Pathway enrichment analysis was done with g:Profiler (http://biit.cs.ut.ee/gprofiler). Upstream regulator analysis was performed with the Ingenuity Pathway Analysis tool (Qiagen, USA).

Metabolomics

The targeted metabolomics approach was based on LC-ESI-MS/MS and FIA-ESI-MS/MS measurements acquired using an AbsoluteIDQ p180 kit (BIOCRATES Life Sciences AG, Austria). Metabolites were quantified from 10 µL plasma samples and the assay was performed as previously described (17). Statistical analysis was performed on 176 metabolites and 50 ratios in MeV (MultiExperiment Viewer, 4.9.0) using a Wilcoxon-Mann-Whitney test with FDR<10% calculated by the Benjamini-Hochberg method.

Histochemistry

Gastrocnemius muscles were frozen and 9 µm cryosections were stained for complex II and IV activities as described earlier (18). Pancreata were fixed in 4% paraformaldehyde and embedded in paraffin blocks. Consecutive 7 µm sections were stained with hematoxylin and eosin using standard procedures. Imaging was performed using a Zeiss Axioplan 2 microscope (Zeiss, Germany).

Immunofluorescence staining

Pancreata were fixed in 4% paraformaldehyde and incubated in solutions with increasing sucrose concentrations (9-30%) before embedding in Tissue Tek (VWR, Germany). Cryosections (7 µm thickness) were cut with 300 µm distances between sections and 3 independent areas/animal were stained with anti-insulin (#180067) or anti-glucagon (#180064) antibodies and with corresponding fluorescent-labeled secondary antibodies. Antibodies were purchased from Invitrogen (Life Technologies, Germany), except anti-GLUT2 (Abcam, UK); DAPI was used to visualize cell nuclei. Slides were scanned using a NanoZoomer 2.0 HT (Hamamatsu, Japan) fluorescence scanner; pancreatic islets (11-92 islets/animal) were evaluated using Definiens Developer XD 2 image analysis software (Definiens AG, Germany).

Transmission electron microscopy

Quadriceps muscles or liver samples were analyzed as described earlier (15).

Western blot

Quadriceps muscles were pulverized in liquid nitrogen and dissolved in HEPES buffer supplemented with protease and phosphatase inhibitors. Antibodies were purchased from Cell Signaling Technology (USA) and western blots were performed as described earlier (19).

Statistics

Statistical evaluations were performed using GraphPad Prism 6.07. Unless otherwise indicated, ANOVA with post hoc Holm-Šídák's multiple comparison tests was used to calculate statistical significance, which was assumed as $p<0.05$.

Results

BEZ does not change mitochondrial function in skeletal muscle

We previously found an impairment of mitochondrial respiration in skeletal muscle from STZ mice (10). To restore mitochondrial dysfunction, STZ mice were treated with 0.5% BEZ

before mitochondrial capacity was analyzed in skeletal muscle. BEZ treatment of STZ mice did not enhance mitochondrial gene expression or complex II and IV staining, and mitochondrial oxygen consumption in muscle was not affected (Suppl. Fig. 1A-C). We also assessed whether BEZ treatment of mice could induce rhabdomyolysis (20), a rare side effect described in human studies. Measurement of rhabdomyolysis-related factors showed no effect of BEZ treatment (Suppl. Fig. 1D-F), suggesting that BEZ did not induce rhabdomyolysis.

BEZ ameliorates impaired glucose metabolism by improving systemic insulin sensitivity

As expected, 0.5% BEZ treatment caused a significant decrease in plasma TG and NEFA levels in STZ mice (Fig. 1A-B). Interestingly, relative to untreated STZ mice, 0.5% BEZ also significantly reduced blood glucose concentrations by 45% and 40% in fasted (Fig. 1C) and random fed conditions (Fig. 1D), respectively. A reduced BEZ dose (0.25%) could also significantly reduce hyperglycemia, plasma TG and NEFA levels (Suppl. Table 2). In all later experiments 0.5% BEZ was used. The improved glycemic control in BEZ-treated versus untreated STZ mice was reflected by a 28% reduction in HbA1c levels (Fig. 1E). Meanwhile, BEZ treatment had no effect on the low insulin levels in STZ, SD mice but decreased circulating insulin levels in control mice (Fig. 1F).

The QUICKI index, a well-established marker for insulin sensitivity, was increased in both BEZ-treated groups (Fig. 2A). Since these findings suggest that BEZ treatment may improve systemic insulin sensitivity, we next determined glucose and insulin tolerance. BEZ treatment significantly improved glucose and insulin tolerance in both control and STZ mice (Fig. 2B-E), indicating that the insulin sensitizing actions of BEZ are independent of hyperglycemia. In *quadriceps* muscle, BEZ elevated levels of phosphorylated AKT, a key component of insulin signaling (Fig. 2F and Supp. Fig. 2A-B). These data suggest that BEZ treatment

improves both muscle and systemic insulin sensitivity that in turn ameliorates the impaired glucose metabolism of STZ mice.

BEZ treatment improves islet morphology and increases islet number

Since pancreatic endocrine cells play a central role in glucose metabolism, we analyzed pancreata sections from STZ mice. Hematoxylin and eosin staining showed that islet structure was severely damaged in STZ mice, whereas BEZ treatment exhibited a protective effect on islet morphology (Fig. 3A). STZ mice had fewer beta-cells compared to healthy controls, and relative to untreated STZ mice BEZ-treated mice tended to increase beta-cell area by 29% as well as islet numbers by 56% (Fig. 3B-E). BEZ did also elevate the diminished GLUT2 staining, which is another important beta-cell marker (Suppl. Fig. 3). To assess whether BEZ suppresses apoptosis in beta-cells, we used staining with anti-caspase-3 as an apoptotic marker; however, BEZ treatment did not decrease the number of caspase-3 positive beta-cells (data not shown). Taken together, these data, although not statistically significant, suggest that BEZ exerts a beneficial effect on islets and especially on beta-cell areas. Anti-CD45R staining revealed no elevated levels of immune cells in pancreata from STZ mice (data not shown), suggesting that inflammation in the pancreas did not occur.

BEZ treatment enhances metabolic flexibility in STZ mice

In order to assess whether improved insulin sensitivity following BEZ treatment was due to altered body composition, the body weight and fat mass were determined. In healthy mice, BEZ treatment reduced the body weight and fat mass (Fig. 4A-C and Suppl. Fig. 4A-C). However, in STZ mice BEZ-mediated effects were not caused by changes in body composition or body weight (Fig. 4A-C and Suppl. Fig. 4A-C). Body weight normalized linear regression of fat or lean mass did not differ among the analyzed groups (Suppl. Fig. 4D-E).

Since low metabolic flexibility is a hallmark of disturbed glucose homeostasis (21), we next performed indirect calorimetry (Fig. 4D-F). BEZ-treated STZ mice displayed a significantly lower respiratory exchange ratio (RER) during the first half of the dark phase and an elevated RER in the second light phase when compared to untreated STZ mice (Fig. 4D). Cumulative food intake curves (Fig. 4E) outlined that the lower RER observed during the first half of the dark phase resulted from a marked delay in food intake in BEZ-treated STZ mice. In contrast, the marked increments in RER in BEZ-treated STZ mice during the second light phase could not be attributed to a difference in food intake when compared to untreated STZ mice (Fig. 4E and Suppl. Fig. 4F-G). Metabolic flexibility, determined by calculating the change in RER (21) between dark and light phases, was lower in STZ, SD mice but increased upon BEZ treatment in both groups (Fig. 4F). BEZ did not significantly change the average oxygen consumption, carbon dioxide production, running distance and rearing activity (Suppl. Fig. 5), suggesting that BEZ did not affect the energy expenditure or activity of STZ mice.

BEZ induces PPAR-regulated, peroxisomal and mitochondrial gene expression programs

To examine activation of PPAR transcription factors by BEZ treatment in liver, microarray analysis was performed. BEZ treatment of STZ mice significantly changed the expression of 3,603 genes (FDR<10%) that displayed at least a ±20% change compared to STZ, SD animals. Among the 1,808 genes that were significantly upregulated, genes in the "PPAR signaling pathway" ($p=2.7x10^{-15}$) and genes related to peroxisomes ($p=4.6x10^{-25}$) were significantly enriched. Notably, genes related to mitochondria ($p=1.8x10^{-49}$) were also enriched, indicating that BEZ treatment may promote both peroxisomal and mitochondrial proliferation.

STZ treatment suppresses insulin target genes and induces inflammatory genes, whereas both pathways are normalized upon BEZ treatment

The expression of genes regulating fatty acid oxidation in the liver was significantly elevated by BEZ treatment (Suppl. Table 3), suggesting elevated fatty acid oxidation via PPAR activation. To determine which PPAR was activated by BEZ treatment in STZ mouse livers (STZ, BEZ vs. STZ, SD), the 3,603 genes that showed significantly altered expression were analyzed by upstream regulator analysis using Ingenuity Pathway Analysis. The positive z-scores calculated by this analysis suggested that all PPARs were induced upon BEZ treatment (Table 1). To analyze the effect of STZ on hepatic gene regulation, microarray data from our previous study (16) were re-evaluated and compared to healthy control animals. STZ treatment significantly changed the expression of 1,771 genes (FDR<10%) that displayed at least a ±20% change compared to healthy control animals. Upstream regulator analysis using these genes suggested a suppression of all PPARs in STZ mice, as represented by negative z-scores (Table 1). STZ treatment was also associated with reduced expression of insulin target genes and elevated expression of inflammatory genes in the liver, whereas BEZ treatment counteracted these STZ-mediated effects (Table 1). These results were supported by real-time PCR data (Suppl. Fig. 6A-B). Furthermore, plasma concentrations of the pro-inflammatory marker CRP were significantly lower in BEZ-treated STZ animals compared to the STZ, SD group (1.38 ± 0.40 vs. 4.97 ± 1.17, respectively; p=0.0003). Taken together, our data suggest that induced expression of PPAR and insulin target genes in parallel with the suppression of inflammatory gene expression in the liver could promote BEZ-dependent improvements in hyperglycemia.

BEZ ameliorates dyslipidemia in STZ mice

Since lipids act as mediators of insulin resistance to play crucial roles in cellular metabolism (7), we assessed a comprehensive plasma lipid profile in BEZ-treated animals (Suppl. Table 5). STZ treatment significantly changed levels of 85 metabolites and metabolite ratios compared to untreated controls. Moreover, BEZ treatment of STZ mice significantly altered

78 metabolites and ratios compared to STZ, SD mice, while 54 metabolites and ratios were common in both comparisons, and 52 showed inverse fold-changes (Table 2, Suppl. Table 4). STZ-treated mice displayed higher acylcarnitine and lower lysophosphatidylcholine (LPC) plasma levels compared to healthy controls, whereas BEZ reduced acylcarnitine and elevated LPC levels compared to untreated STZ mice (Table 2). In STZ mice the ratios of monounsaturated fatty acids (MUFA) to saturated fatty acids (SFA) and total LPC levels were lower, whereas BEZ treatment normalized these ratios (Table 2). Furthermore, hexose (H1), which mainly represents glucose in the plasma, was significantly higher in STZ mice and decreased after BEZ treatment, which was consistent with blood glucose measurements (Fig. 1C-D). Many changes in levels of phosphatidylcholines (PC), sphingomyelines (SM) and amino acids were also significantly reverted upon BEZ treatment (Suppl. Table 4).

BEZ increases mitochondrial mass and capacity in liver

BEZ treatment increased the number of mitochondria and decreased the number of lipid droplets in livers of control and STZ mice compared to their respective untreated controls (Fig. 5A). Furthermore, BEZ treatment elevated mitochondrial gene expression compared to STZ, SD mice (Suppl. Fig. 6C), but did not affect mitochondrial mass in skeletal muscle (Suppl. Fig. 2C). BEZ treatment also increased oxygen consumption in livers from both healthy and STZ mice (Fig. 5B-C). Since equal amounts of mitochondrial protein were used in the oxygen consumption experiments, these findings suggest that BEZ treatment not only promoted elevated mitochondrial mass in the liver by increasing the expression of genes encoding mitochondrial proteins, but also enhances mitochondrial function.

Next, we analyzed whether BEZ could ameliorate the disturbed mitochondrial function in human fibroblasts isolated from patients with mitochondrial complex I deficiency resulting from mutations in genes encoding different complex I subunits or Acyl-CoA dehydrogenase 9 (ACAD9). BEZ treatment significantly elevated complex I-driven respiration in almost all

fibroblast samples (Fig. 5D), and also enhanced mitochondrial respiration via complex II and IV substrates (Suppl. Fig. 7).

Discussion

Several studies suggest that BEZ decreases blood glucose levels in rodent models of type 1 and type 2 diabetes (22,23). In combination with other anti-diabetic medications, BEZ has already been shown in 1978 to improve hyperglycemia in patients with type 2 diabetes (24), which was confirmed by several independent studies later (6,25). Two studies reported significantly lower blood glucose levels in type 1 diabetes patients treated with BEZ (26,27), which was not obvious later (28). Consistent with the above-mentioned studies here we observed a marked reduction in blood glucose levels in insulin-deficient STZ mice (Fig. 1C-D), suggesting that BEZ indeed has an anti-diabetic effect in rodents. Furthermore, BEZ treatment reduced high HbA1c levels in STZ mice (Fig. 1E), which was also shown in type 2 diabetes patients (25), and indicates a long-term benefit of BEZ treatment on glycemic control. BEZ treatment also elevated QUICKI in both treatment groups (Fig. 2A), suggesting that it can enhance insulin sensitivity. A similar improvement in the insulin sensitivity index was reported in patients with high lipid levels (29). Furthermore, BEZ improved glucose tolerance in patients with type 2 diabetes or high lipid levels (6,25,29). BEZ treatment also improved glucose and insulin tolerance in STZ mice (Fig. 2B-E), which was previously reported for rodent models of type 2 diabetes (22). Moreover, we observed a higher p-AKT/AKT ratio in skeletal muscle upon BEZ treatment (Fig. 2F), indicating improved muscle insulin sensitivity. Induction of inflammatory pathways was postulated to induce diabetes by attenuating insulin sensitivity and several anti-inflammatory therapies were demonstrated to efficiently improve diabetes (30). BEZ treatment counteracted the elevated expression of inflammatory genes and at the same time the suppressed expression of insulin target genes in the liver of STZ mice (Table 1). These data suggest that BEZ could indeed

have anti-inflammatory effects, as was previously reported by others (31,32), and may thereby improve insulin sensitivity.

Decreased plasma acylcarnitine levels were found in BEZ treated STZ animals, which could also reflect improved beta-oxidation (33). Since BEZ was recently shown to affect plasma LPC levels (34), and LPCs can in turn regulate glucose uptake (35), the enhanced LPC levels observed following BEZ treatment could increase glucose uptake in the treated mice. In addition, the increased MUFA/SFA ratios could be associated with the improved insulin sensitivity (36). Taken together, we assume that the enhanced whole body insulin sensitivity contributes to improved glucose tolerance.

BEZ belongs to the group of fibrates, which are known activators of PPARα (37) and decrease cardiovascular risk in diabetes patients (3). BEZ is unique among fibrates as it is the only known pan-PPAR activator (37,38). Indeed, our data indicate that all PPARs, but particularly PPARα, were upregulated in the BEZ-treated animals (Table 1). PPARα induction could be involved in ameliorated glucose metabolism and insulin sensitivity by decreasing levels of circulating lipids through higher expression of genes involved in fatty acid oxidation in the liver. Meanwhile, PPARγ activation is known to increase glucose uptake in muscle and fat tissues, and also has anti-inflammatory properties and the ability to reduce glucose synthesis in the liver (38). PPARγ pathways could participate in the ameliorated glucose metabolism in our mice and are consistent with the increased muscle p-AKT/AKT ratio, as well as with the decreased expression of inflammatory genes and increased expression of insulin target genes in the liver. However, less is known about PPARδ function, the activation of which is implicated in higher fatty acid oxidation, increased energy consumption and adaptive thermogenesis (37). Our data suggest that, in addition to PPARα, PPARγ and PPARδ were also activated in the liver following BEZ treatment of STZ mice,

thus verifying the pan-activator activity of BEZ, and highlighting the clear benefit of BEZ relative to other fibrates that activate PPARα. Since all three PPARs were downregulated in STZ mice, the activation all of them is likely needed to provide a beneficial effect of BEZ on glucose metabolism in STZ mice.

To investigate whether BEZ causes rhabdomyolysis, a rare side effect found in human studies (1), rhabdomyolysis-associated factors (20) were measured in plasma from BEZ-treated mice. None of the tested factors was significantly changed in the BEZ-treated animals (Suppl. Fig. 1D-F), suggesting that rhabdomyolysis did not occur. This outcome is consistent with previous studies that showed no rhabdomyolysis following BEZ treatment at the same dosage (9,20,39). We found that BEZ, like other fibrates, can induce hepatomegaly in mice (data not shown), which is consistent with previous studies (40), and may be attributable to its capacity to induce peroxisome proliferation (41). Peroxisomal proliferation is species-specific (42,43) because fibrate treatment does not cause hepatomegaly and peroxisomal proliferation in primates and humans (44-46). The 0.5% BEZ dose used in our study was chosen according to three previous, independent mouse studies (9,20,39). On the other hand, the applied dose in mice is higher than that given to humans in clinical studies wherein BEZ dosages were normalized to body weights (42). Since mice have higher metabolic turnover and a much smaller body surface area than humans (47), the human equivalent dose was calculated for the applied BEZ dose. According to this calculation (47), 0.5% BEZ is equivalent to 67 mg/kg in humans, which is higher but still in the range of routine doses used in human studies (10 mg/kg, (6,8)). We also confirmed that a 0.25% BEZ dose could significantly decrease hyperglycemia in STZ mice (Suppl. Table 2).

Insulin resistance and mitochondrial dysfunction are intimately related (48) and mitochondrial dysfunction can occur in insulin resistant states (10,49). Improving

mitochondrial function seems to play a role in ameliorating insulin resistance (50). After BEZ treatment of STZ mice we observed a marked increase in hepatic mitochondrial mass and respiration capacity (Fig. 5A-C) that was accompanied by improved insulin sensitivity (Fig. 2D-F and Table 1).

Furthermore, BEZ treatment of fibroblasts from patients having complex I or ACAD9 mutations elevated mitochondrial respiration (Fig. 5D and Suppl. Fig. 7), suggesting that BEZ could reverse diminished mitochondrial function, which was reported for other mitochondrial mutations (8) and is shown for the first time in our study for patients with ACAD9 mutations. Myoblasts isolated from patients with mitochondrial *CPT2* gene mutations who were treated with BEZ showed elevated *CPT1b*, *CPT2* mRNA levels, whereas mitochondria isolated from these patients displayed higher palmitate respiration rates (8,51), which is in line with the elevated mitochondrial oxygen consumption seen in our fibroblast cell lines (Fig. 5D and Suppl. Fig. 7). The liver microarray and real-time PCR data showed higher mRNA levels for *CPT1b* and *CPT2* in STZ mice upon BEZ treatment (Suppl. Table 3, Suppl. Fig. 6C). Bastin et al. showed elevated mitochondrial gene expression in fibroblasts isolated from patients with deficiencies in mitochondrial complexes following BEZ treatment (52) as we have also observed higher mRNA levels of genes encoding mitochondrial complexes in livers of BEZ-treated STZ mice (Suppl. Fig. 6C). These data suggest that BEZ treatment likely enhances the gene expression of mitochondrial proteins and oxygen consumption through similar pathways in humans and in mice.

Since mitochondria play a central role in cellular metabolism by oxidizing different available substrates for ATP production (53), mitochondrial dysfunction is likely involved in metabolic inflexibility (21). BEZ treatment improved metabolic flexibility (Fig. 4F) probably by increasing fatty acid (Suppl. Table 3) and glucose oxidation (Fig. 4D). Improved metabolic flexibility in turn could decrease both NEFA and blood glucose levels in STZ mice

(Fig. 1B, D). BEZ-treated patients carrying the *PNPLA2* mutation also show ameliorated metabolic flexibility in parallel with improved mitochondrial function and insulin sensitivity (54), suggesting that enhanced metabolic flexibility could have clinical relevance in BEZ therapies.

Our data suggest that BEZ enhances hepatic mitochondrial performance and insulin sensitivity, which could ameliorate metabolic inflexibility and insulin resistance that in turn preserves beta-cell area and insulin action to improve glucose metabolism and hyperglycemia in STZ mice (Fig. 5E). Our and previous studies also indicate that glucose metabolism and the underlying molecular pathways involving mitochondrial function are comparable between mice and humans and could be similarly regulated by BEZ application. The beneficial actions of BEZ on glucose metabolism in addition to its effects in hyperlipidemia patients, suggest that BEZ could also be useful for treating patients with impaired glucose tolerance or diabetes.

Acknowledgements

An.Fr. conceived the experiments, researched the data, contributed to discussions and wrote the manuscript. P.H. contributed to the analysis, discussions and wrote the manuscript. M.I., Bi.Ra., M.B., M.A., An.Fe., P.S., researched the data and edited/reviewed the manuscript. J.R., G.D., R.M., D.G., O.S., C.S.L., F.N., C.P. and Bi.Re. researched the data. J.B., A.K.W., H.F., E.W., S.N., G.K.H.P., J.A., A.P. edited/reviewed the manuscript. H.P., M.S., R.J.W. and M.H.d.A. conceived the experiments, contributed to discussions and edited/reviewed the manuscript. M.H.d.A is the guarantor of this work and, as such, had full access to all the data in the study and takes responsibility for the integrity of the data and the accuracy of the data analysis. The authors declare that there are no conflicts of interest.

This work was supported by a grant from the German Federal Ministry of Education and Research (BMBF) to the German Center for Diabetes Research (DZD e.V.) and Infrafrontier (German Mouse Clinic) and by grants from the Helmholtz Portfolio Theme 'Metabolic Dysfunction and Common Disease' (J.B.) and the Helmholtz Alliance 'Imaging and Curing Environmental Metabolic Diseases, ICEMED' (J.B.). We thank Michael Schulz (Institute of Experimental Genetics, Helmholtz Zentrum München) for excellent technical assistance and Dr. Robert Brommage (German Mouse Clinic, Helmholtz Zentrum München) for valuable comments on the manuscript.

References

1. Tenenbaum A, Fisman EZ, Motro M, Adler Y: Optimal management of combined dyslipidemia: what have we behind statins monotherapy? Adv Cardiol 2008;45:127-153
2. Ohno Y, Miyoshi T, Noda Y, Oe H, Toh N, Nakamura K, Kohno K, Morita H, Ito H: Bezafibrate improves postprandial hypertriglyceridemia and associated endothelial dysfunction in patients with metabolic syndrome: a randomized crossover study. Cardiovasc Diabetol 2014;13:71
3. Klempfner R, Goldenberg I, Fisman EZ, Matetzky S, Amit U, Shemesh J, Tenenbaum A: Comparison of statin alone versus bezafibrate and statin combination in patients with diabetes mellitus and acute coronary syndrome. Am J Cardiol 2014;113:12-16
4. Grygiel-Gorniak B: Peroxisome proliferator-activated receptors and their ligands: nutritional and clinical implications--a review. Nutrition journal 2014;13:17
5. Flory JH, Ellenberg S, Szapary PO, Strom BL, Hennessy S: Antidiabetic action of bezafibrate in a large observational database. Diabetes Care 2009;32:547-551
6. Jones IR, Swai A, Taylor R, Miller M, Laker MF, Alberti KG: Lowering of plasma glucose concentrations with bezafibrate in patients with moderately controlled NIDDM. Diabetes Care 1990;13:855-863
7. Jelenik T, Roden M: Mitochondrial plasticity in obesity and diabetes mellitus. Antioxidants & redox signaling 2013;19:258-268
8. Bonnefont JP, Bastin J, Behin A, Djouadi F: Bezafibrate for an inborn mitochondrial beta-oxidation defect. N Engl J Med 2009;360:838-840
9. Wenz T, Diaz F, Spiegelman BM, Moraes CT: Activation of the PPAR/PGC-1alpha pathway prevents a bioenergetic deficit and effectively improves a mitochondrial myopathy phenotype. Cell Metab 2008;8:249-256
10. Franko A, von Kleist-Retzow JC, Bose M, Sanchez-Lasheras C, Brodesser S, Krut O, Kunz WS, Wiedermann D, Hoehn M, Stohr O, Moll L, Freude S, Krone W, Schubert M, Wiesner RJ: Complete failure of insulin-transmitted signaling, but not obesity-induced insulin resistance, impairs respiratory chain function in muscle. J Mol Med (Berl) 2012;90:1145-1160
11. Fuchs H, Neschen S, Rozman J, Rathkolb B, Wagner S, Adler T, Afonso L, Aguilar-Pimentel J, Becker L, Bohla A, Calzada-Wack J, Cohrs C, Frankó A, Garrett L, Glasl L, Götz A, Hagn M, Hans W, Hölter S, Horsch M, Kahle M, Kistler M, Klein-Rodewald T, Lengger C, Ludwig T, Maier H, Marschall S, Micklich K, Möller G, Naton B, Neff F, Prehn C, Puk O, Rácz I, Räß M, Scheerer M, Schiller E, Schöfer F, Schrewe A, Steinkamp R, Stöger C, Treise I, Willershäuser M, Wolff-Muscate A, Zeh R, Adamski J, Beckers J, Bekeredjian R, Busch D, Esposito I, Favor J, Graw J, Katus H, Klopstock T, Ollert M, Schulz H, Stöger T, Wurst W, Yildirim A, Zimmer A, Wolf E, Klingenspor M, Gailus-Durner V, Hrabě de Angelis M: Mouse genetics and metabolic mouse phenotyping. In *Genetics Meets Metabolomics: from Experiment to Systems Biology* Suhre K, Ed. Springer New York, Springer Science+Business Media, LLC, 2012, p. 85-106
12. Haack TB, Danhauser K, Haberberger B, Hoser J, Strecker V, Boehm D, Uziel G, Lamantea E, Invernizzi F, Poulton J, Rolinski B, Iuso A, Biskup S, Schmidt T, Mewes HW, Wittig I, Meitinger T, Zeviani M, Prokisch H: Exome sequencing identifies ACAD9 mutations as a cause of complex I deficiency. Nat Genet 2010;42:1131-1134
13. Haack TB, Madignier F, Herzer M, Lamantea E, Danhauser K, Invernizzi F, Koch J, Freitag M, Drost R, Hillier I, Haberberger B, Mayr JA, Ahting U, Tiranti V, Rotig A, Iuso A, Horvath R, Tesarova M, Baric I, Uziel G, Rolinski B, Sperl W, Meitinger T, Zeviani M, Freisinger P, Prokisch H: Mutation screening of 75 candidate genes in 152 complex I

deficiency cases identifies pathogenic variants in 16 genes including NDUFB9. J Med Genet 2012;49:83-89
14. Gerards M, van den Bosch BJ, Danhauser K, Serre V, van Weeghel M, Wanders RJ, Nicolaes GA, Sluiter W, Schoonderwoerd K, Scholte HR, Prokisch H, Rotig A, de Coo IF, Smeets HJ: Riboflavin-responsive oxidative phosphorylation complex I deficiency caused by defective ACAD9: new function for an old gene. Brain 2011;134:210-219
15. Franko A, Baris OR, Bergschneider E, von Toerne C, Hauck SM, Aichler M, Walch AK, Wurst W, Wiesner RJ, Johnston IC, de Angelis MH: Efficient Isolation of Pure and Functional Mitochondria from Mouse Tissues Using Automated Tissue Disruption and Enrichment with Anti-TOM22 Magnetic Beads. PLoS One 2013;8:e82392
16. Franko A, von Kleist-Retzow JC, Neschen S, Wu M, Schommers P, Bose M, Kunze A, Hartmann U, Sanchez-Lasheras C, Stoehr O, Huntgeburth M, Brodesser S, Irmler M, Beckers J, de Angelis MH, Paulsson M, Schubert M, Wiesner RJ: Liver adapts mitochondrial function to insulin resistant and diabetic states in mice. J Hepatol 2014;60:816-823
17. Zukunft S, Sorgenfrei M, Prehn C, Möller G, Adamski J: Targeted Metabolomics of Dried Blood Spot Extracts. Chromatographia 2013;76:1295-1305
18. Zsurka G, Schroder R, Kornblum C, Rudolph J, Wiesner RJ, Elger CE, Kunz WS: Tissue dependent co-segregation of the novel pathogenic G12276A mitochondrial tRNALeu(CUN) mutation with the A185G D-loop polymorphism. J Med Genet 2004;41:e124
19. Stohr O, Hahn J, Moll L, Leeser U, Freude S, Bernard C, Schilbach K, Markl A, Udelhoven M, Krone W, Schubert M: Insulin receptor substrate-1 and -2 mediate resistance to glucose-induced caspase-3 activation in human neuroblastoma cells. Biochim Biophys Acta 2011;1812:573-580
20. Viscomi C, Bottani E, Civiletto G, Cerutti R, Moggio M, Fagiolari G, Schon EA, Lamperti C, Zeviani M: In vivo correction of COX deficiency by activation of the AMPK/PGC-1alpha axis. Cell Metab 2011;14:80-90
21. Galgani JE, Moro C, Ravussin E: Metabolic flexibility and insulin resistance. Am J Physiol Endocrinol Metab 2008;295:E1009-1017
22. Jia D, Yamamoto M, Otani M, Otsuki M: Bezafibrate on lipids and glucose metabolism in obese diabetic Otsuka Long-Evans Tokushima fatty rats. Metabolism 2004;53:405-413
23. Anwer T, Sharma M, Pillai KK, Haque SE, Alam MM, Zaman MS: Protective effect of bezafibrate on streptozotocin-induced oxidative stress and toxicity in rats. Toxicology 2007;229:165-172
24. Wahl P, Hasslacher C, Lang PD, Vollmar J: [Lipid-lowering effect of bezafibrate in patients with diabetes mellitus and hyperlipidaemia (author's transl)]. Dtsch Med Wochenschr 1978;103:1233-1237
25. Ogawa S, Takeuchi K, Sugimura K, Fukuda M, Lee R, Ito S, Sato T: Bezafibrate reduces blood glucose in type 2 diabetes mellitus. Metabolism 2000;49:331-334
26. Winocour PH, Durrington PN, Bhatnagar D, Ishola M, Arrol S, Lalor BC, Anderson DC: Double-blind placebo-controlled study of the effects of bezafibrate on blood lipids, lipoproteins, and fibrinogen in hyperlipidaemic type 1 diabetes mellitus. Diabet Med 1990;7:736-743
27. Durrington PN, Winocour PH, Bhatnagar D: Bezafibrate retard in patients with insulin-dependent diabetes: effect on serum lipoproteins, fibrinogen, and glycemic control. J Cardiovasc Pharmacol 1990;16 Suppl 9:S30-34
28. Winocour PH, Durrington PN, Bhatagnar D, Ishola M, Mackness M, Arrol S, Anderson DC: The effect of bezafibrate on very low density lipoprotein (VLDL), intermediate density lipoprotein (IDL), and low density lipoprotein (LDL) composition in type 1 diabetes associated with hypercholesterolaemia or combined hyperlipidaemia. Atherosclerosis 1992;93:83-94

29. Kim JI, Tsujino T, Fujioka Y, Saito K, Yokoyama M: Bezafibrate improves hypertension and insulin sensitivity in humans. Hypertens Res 2003;26:307-313
30. Goldfine AB, Fonseca V, Shoelson SE: Therapeutic approaches to target inflammation in type 2 diabetes. Clin Chem 2011;57:162-167
31. Nagasawa T, Inada Y, Nakano S, Tamura T, Takahashi T, Maruyama K, Yamazaki Y, Kuroda J, Shibata N: Effects of bezafibrate, PPAR pan-agonist, and GW501516, PPARdelta agonist, on development of steatohepatitis in mice fed a methionine- and choline-deficient diet. Eur J Pharmacol 2006;536:182-191
32. Jonkers IJ, Mohrschladt MF, Westendorp RG, van der Laarse A, Smelt AH: Severe hypertriglyceridemia with insulin resistance is associated with systemic inflammation: reversal with bezafibrate therapy in a randomized controlled trial. Am J Med 2002;112:275-280
33. Adams SH, Hoppel CL, Lok KH, Zhao L, Wong SW, Minkler PE, Hwang DH, Newman JW, Garvey WT: Plasma acylcarnitine profiles suggest incomplete long-chain fatty acid beta-oxidation and altered tricarboxylic acid cycle activity in type 2 diabetic African-American women. J Nutr 2009;139:1073-1081
34. Takahashi H, Goto T, Yamazaki Y, Kamakari K, Hirata M, Suzuki H, Shibata D, Nakata R, Inoue H, Takahashi N, Kawada T: Metabolomics reveal 1-palmitoyl lysophosphatidylcholine production by peroxisome proliferator-activated receptor alpha. J Lipid Res 2015;56:254-265
35. Yea K, Kim J, Yoon JH, Kwon T, Kim JH, Lee BD, Lee HJ, Lee SJ, Kim JI, Lee TG, Baek MC, Park HS, Park KS, Ohba M, Suh PG, Ryu SH: Lysophosphatidylcholine activates adipocyte glucose uptake and lowers blood glucose levels in murine models of diabetes. J Biol Chem 2009;284:33833-33840
36. Silbernagel G, Kovarova M, Cegan A, Machann J, Schick F, Lehmann R, Haring HU, Stefan N, Schleicher E, Fritsche A, Peter A: High hepatic SCD1 activity is associated with low liver fat content in healthy subjects under a lipogenic diet. J Clin Endocrinol Metab 2012;97:E2288-2292
37. Tenenbaum A, Fisman EZ: Balanced pan-PPAR activator bezafibrate in combination with statin: comprehensive lipids control and diabetes prevention? Cardiovasc Diabetol 2012;11:140
38. Zafrir B, Jain M: Lipid-lowering therapies, glucose control and incident diabetes: evidence, mechanisms and clinical implications. Cardiovasc Drugs Ther 2014;28:361-377
39. Yatsuga S, Suomalainen A: Effect of bezafibrate treatment on late-onset mitochondrial myopathy in mice. Hum Mol Genet 2012;21:526-535
40. Pill J, Kuhnle HF: BM 17.0744: a structurally new antidiabetic compound with insulin-sensitizing and lipid-lowering activity. Metabolism 1999;48:34-40
41. Fahimi HD, Beier K, Lindauer M, Schad A, Zhan J, Pill J, Rebel W, Volkl A, Baumgart E: Zonal heterogeneity of peroxisome proliferation in rat liver. Ann N Y Acad Sci 1996;804:341-361
42. Djouadi F, Bastin J: Species differences in the effects of bezafibrate as a potential treatment of mitochondrial disorders. Cell Metab 2011;14:715-716; author reply 717
43. Dillon LM, Hida A, Garcia S, Prolla TA, Moraes CT: Long-term bezafibrate treatment improves skin and spleen phenotypes of the mtDNA mutator mouse. PLoS One 2012;7:e44335
44. de la Iglesia F, McGuire EJ, Haskins JR, Lalwani ND: Structural diversity of peroxisome proliferators and their effects on mammalian liver cells in vivo. Ann N Y Acad Sci 1996;804:310-327
45. Fahimi HD, Baumgart E, beier K, Pill J, Hartig F, Völkl A: Ultrastructural and biochemical aspects of peroxisome proliferation and biogenesis in different mammalian

species. In *Peroxisomes: Biology and Importance in Toxicology and Medicine* Brian GL, Gordon G, Eds. London, Taylor and Francis, 1993, p. 395-424
46. De La Iglesia FA, Lewis JE, Buchanan RA, Marcus EL, McMahon G: Light and electron microscopy of liver in hyperlipoproteinemic patients under long-term gemfibrozil treatment. Atherosclerosis 1982;43:19-37
47. Reagan-Shaw S, Nihal M, Ahmad N: Dose translation from animal to human studies revisited. FASEB J 2008;22:659-661
48. Montgomery MK, Turner N: Mitochondrial dysfunction and insulin resistance: an update. Endocr Connect 2015;4:R1-R15
49. Sleigh A, Raymond-Barker P, Thackray K, Porter D, Hatunic M, Vottero A, Burren C, Mitchell C, McIntyre M, Brage S, Carpenter TA, Murgatroyd PR, Brindle KM, Kemp GJ, O'Rahilly S, Semple RK, Savage DB: Mitochondrial dysfunction in patients with primary congenital insulin resistance. J Clin Invest 2011;121:2457-2461
50. Zhang LN, Zhou HY, Fu YY, Li YY, Wu F, Gu M, Wu LY, Xia CM, Dong TC, Li JY, Shen JK, Li J: Novel small-molecule PGC-1alpha transcriptional regulator with beneficial effects on diabetic db/db mice. Diabetes 2013;62:1297-1307
51. Bonnefont JP, Bastin J, Laforet P, Aubey F, Mogenet A, Romano S, Ricquier D, Gobin-Limballe S, Vassault A, Behin A, Eymard B, Bresson JL, Djouadi F: Long-term follow-up of bezafibrate treatment in patients with the myopathic form of carnitine palmitoyltransferase 2 deficiency. Clin Pharmacol Ther 2010;88:101-108
52. Bastin J, Aubey F, Rotig A, Munnich A, Djouadi F: Activation of peroxisome proliferator-activated receptor pathway stimulates the mitochondrial respiratory chain and can correct deficiencies in patients' cells lacking its components. J Clin Endocrinol Metab 2008;93:1433-1441
53. Franko A, Hrabe De Angelis M, Wiesner RJ: Mitochondrial Function, Dysfunction and Adaptation in the Liver during the Development of Diabetes. In *Mitochondria in Liver Disease* Han D, Kaplowitz N, Eds. Abingdon, UK, CRC Press, 2015, p. 383-411
54. van de Weijer T, Havekes B, Bilet L, Hoeks J, Sparks L, Bosma M, Paglialunga S, Jorgensen J, Janssen MC, Schaart G, Sauerwein H, Smeets JL, Wildberger J, Zechner R, Schrauwen-Hinderling VB, Hesselink MK, Schrauwen P: Effects of bezafibrate treatment in a patient and a carrier with mutations in the PNPLA2 gene, causing neutral lipid storage disease with myopathy. Circ Res 2013;112:e51-54

Table 1 Ingenuity Upstream Regulator analysis predicts that BEZ activates PPARs as well as insulin target genes and reduces mediators of inflammation in the liver

Category	Upstream regulator	z-score of STZ, SD/Con, SD	z-score of STZ, BEZ/STZ, SD
PPAR	PPARα	-1.59	8.30
PPAR	PPARβ/δ	-2.03	2.52
PPAR	PPARγ	-2.85	4.30
insulin sig	Insulin	-1.31	1.35
insulin sig	INSR	-0.96	4.15
insulin sig	IRS1	-1.82	1.52
insulin sig	IRS2	-0.77	1.37
inflammation	TNF	5.62	-3.29
inflammation	IL1β	4.62	-2.29
inflammation	IFNγ	5.34	-5.87
inflammation	IL6	4.98	-3.34
inflammation	OSM	2.41	-3.01
inflammation	pro-infl. cytokines	2.95	-2.16
inflammation	TLR3	4.32	-2.91
inflammation	TLR4	4.21	-2.60

STZ treatment significantly altered the expression of 1,771 genes compared to Con, SD animals. On the other hand, BEZ treatment of STZ mice significantly altered the expression of 3,603 genes compared to STZ, SD mice. These two significantly altered gene groups were analyzed with Ingenuity Pathway Analysis and common, significantly enriched upstream regulators with inverse regulation were identified. Z-scores>0 indicate activation, z-scores<0

indicate inhibition. Values >2 or <-2 indicate significant results, whereas values between -2 and 2 represent trends.

Table 2 Fold changes of plasma metabolite levels (19 out of 52), which show inverse regulation between STZ, BEZ vs. STZ, SD and STZ, SD vs. Con, SD comparisons

Metabolites	STZ, SD/Con, SD	STZ, BEZ/STZ, SD	
C0	-1.8	2.3	
C10	1.6	-1.4	*
C14:2	1.7	-2.4	*
C18	1.6	-2.2	*
C18:2	2.4	-2.5	
C4:1	2.0	-1.5	*
H1	2.4	-1.7	
LPC a C14:0	-1.8	1.3	*
LPC a C16:0	-1.7	1.7	
LPC a C16:1	-8.5	12.0	
LPC a C17:0	1.5	-1.7	
LPC a C18:1	-4.0	5.2	
LPC a C20:3	-4.6	6.9	
LPC a C20:4	-1.5	1.3	
MUFA (PC)	-3.2	3.5	*
MUFA (PC) / SFA (PC)	-2.3	2.8	*
MUFA (LPC)	-4.0	5.3	*
MUFA (LPC) / SFA (LPC)	-2.9	4.0	*
Total LPC	-1.4	1.5	*

STZ treatment significantly altered the level of 85 metabolites and metabolite ratios compared to Con, SD animals (left column). On the other hand, BEZ treatment of STZ mice significantly altered 78 metabolites and metabolite ratios compared to STZ, SD mice (right column). Among these comparisons there were 54 common metabolites and metabolite ratios, with 52 of them showing inverse regulation. Numbers denote fold changes calculated by dividing the appropriate means of groups. Nineteen chosen ratios are shown, the other 33 ratios are given in Suppl. Table 4. The original data are shown in Suppl. Table 5.

C: acylcarnitine, C0: free carnitine, numbers after C denote the length of carbon chain, the numbers after : denote the number of double bounds, H1:hexose, LPC: lysophosphatidyl

choline, MUFA: monounsaturated fatty acid, SFA: saturated fatty acid, PUFA: polyunsaturated fatty acid, PC: phosphatidyl choline. * denotes values, which were lower than 3-times zero values.

Figure legends

Fig. 1 Levels of plasma lipid, insulin, blood glucose and HbA1c in STZ mice

A Plasma triglyceride (TG) and **B** non-esterified fatty acids (NEFA). **C** Fasted, **D** random fed blood glucose (BG) and **E** HbA1c levels. Values under the figure represent IFCC-recommended mean HbA1c data in mmol/mol. **F** Plasma insulin levels. Columns represent averages ± standard deviations; n=5-8. ***** denotes significant differences between STZ, BEZ vs. STZ, SD; *p<0.05, ***p<0.001; **#** denotes significant differences between STZ, SD vs. Con, SD; #p<0.05, ###p<0.001; **§** denotes significant differences between Con, BEZ vs. Con, SD; §p<0.05, §§§p<0.001.

Fig. 2 QUICKI, glucose-, insulin-tolerance tests and muscle p-AKT/AKT ratio in STZ mice

A Quantitative insulin sensitivity check index (QUICKI). **B** Glucose tolerance tests (GTT) and **C** area under the curve (AUC) evaluation. **D** Insulin tolerance tests (ITT) normalized for basal BG and **E** area under the curve (AUC) evaluation. **F** anti-AKT and anti-phospho-473-AKT antibodies were used in western blotting to visualize protein levels from *quadriceps* muscles. Values were densitometrically evaluated (Suppl. Fig. 2A-B) and p-AKT/AKT ratios were built. Columns represent averages ± standard deviations; n=4-8 animals. ***** denotes significant differences between STZ, BEZ vs. STZ, SD; *p<0.05, ***p<0.001; **#** denotes significant differences between STZ, SD vs. Con, SD; ##p<0.01, ###p<0.001; **§** denotes significant differences between Con, BEZ vs. Con, SD; §p<0.05, §§p<0.01, §§§p<0.001.

Fig. 3 Pancreas architecture in STZ mice

A Pancreata were stained with hematoxylin and eosin and visualized by light microscopy. The white bar represents 100 µm. **B** Pancreata were stained with anti-insulin (green) and anti-glucagon (red) antibodies and visualized by fluorescence microscopy. Cell nuclei were stained with DAPI (blue). The white bar represents 50 µm. Representative areas are shown. **C**

Insulin and **D** glucagon area were calculated using Architect software and values were normalized to total pancreas area. **E** Islet number was manually counted and values were normalized to total pancreas area. Columns represent averages ± standard deviations; A represents n=2, B-E represent n=7-8 animals. **#** denotes significant differences between STZ, SD vs. Con, SD; #p<0.05.

Fig. 4 Body composition and indirect calorimetry in STZ mice

A Body weight. **B** Fat and **C** lean mass were measured by qNMR (Suppl. Fig. 4B-C) and normalized to body weights in %. **D** Respiratory exchange ratios (RERs) were calculated by dividing carbon dioxide production (VCO_2) by oxygen consumption (VO_2) (Suppl. Fig. 5A-D). The gray rectangle represents 12 hour dark phase (0 time point represents 3 p.m.). **E** Cumulative food consumption. **F** ΔRER was calculated as RER_{max}-RER_{min}. Columns represent averages ± standard deviations; n=5-8 animals. ***** denotes significant differences between STZ, BEZ vs. STZ, SD; ***p<0.001; **#** denotes significant differences between STZ, SD vs. Con, SD; #p<0.05, ###p<0.001; **§** denotes significant differences between Con, BEZ vs. Con, SD; §§p<0.01, §§§p<0.001.

Fig. 5 Mitochondrial mass in STZ mouse livers and mitochondrial function in BEZ-treated STZ mice and human fibroblasts

A Liver mitochondrial mass and architecture were assessed by transmission EM. Pictures were taken at 1,600x magnification; the white bar denotes 2 μm. Representative areas are shown. **B-C** Oxygen consumption was measured from isolated liver mitochondria with an XF Extracellular Flux Analyzer. **B** Coupling assay, starting with succinate as a substrate for complex II in the absence of adenosine diphosphate (ADP)=basal; the indicated substrates/inhibitors were used. Oligo: oligomycin; FCCP: carbonyl cyanide-4-(trifluoromethoxy)phenylhydrazone **C** Electron flow assay with the indicated substrates, pyr: pyruvate, mal: malate serving as substrates for complex I, succ: succinate, a substrate for

complex II, TMPD: tetramethylphenylendiamin, a substrate for complex IV. **D** Mitochondrial respiration was determined with glutamate and malate as complex I substrates in fibroblasts of patients with complex I deficiency (the loci of the mutation for the appropriate subunits of complex I are indicated under the figure) or ACAD9 mutations. Data are normalized to the lowest value of untreated control samples. **E** Our data demonstrated that BEZ improves glucose metabolism in STZ mice. In this scheme the possible underlying mechanisms are depicted, which are probably involved in the beneficial effects of BEZ. Columns represent averages ± standard deviations; A-C represent n=5-8 animals, D represent values measured from individual fibroblasts. B-C ***** denotes significant differences between STZ, BEZ vs. STZ, SD; *p<0.05, **p<0.01; **#** denotes significant differences between STZ, SD vs. Con, SD; #p<0.05, ##p<0.01, ###p<0.001; **§** denotes significant differences between Con, BEZ vs. Con, SD; §p<0.05. For calculating p-values for B-C, Anova and Holm-Šídák's tests were applied, and for control fibroblasts (n=7-33) and patient fibroblasts (n=3-11) in D, replicates were applied and Student's t-tests were used to calculate p-values. ***** denotes significant differences between BEZ-treated and untreated fibroblasts; *p<0.05, **p<0.01, ***p<0.001.

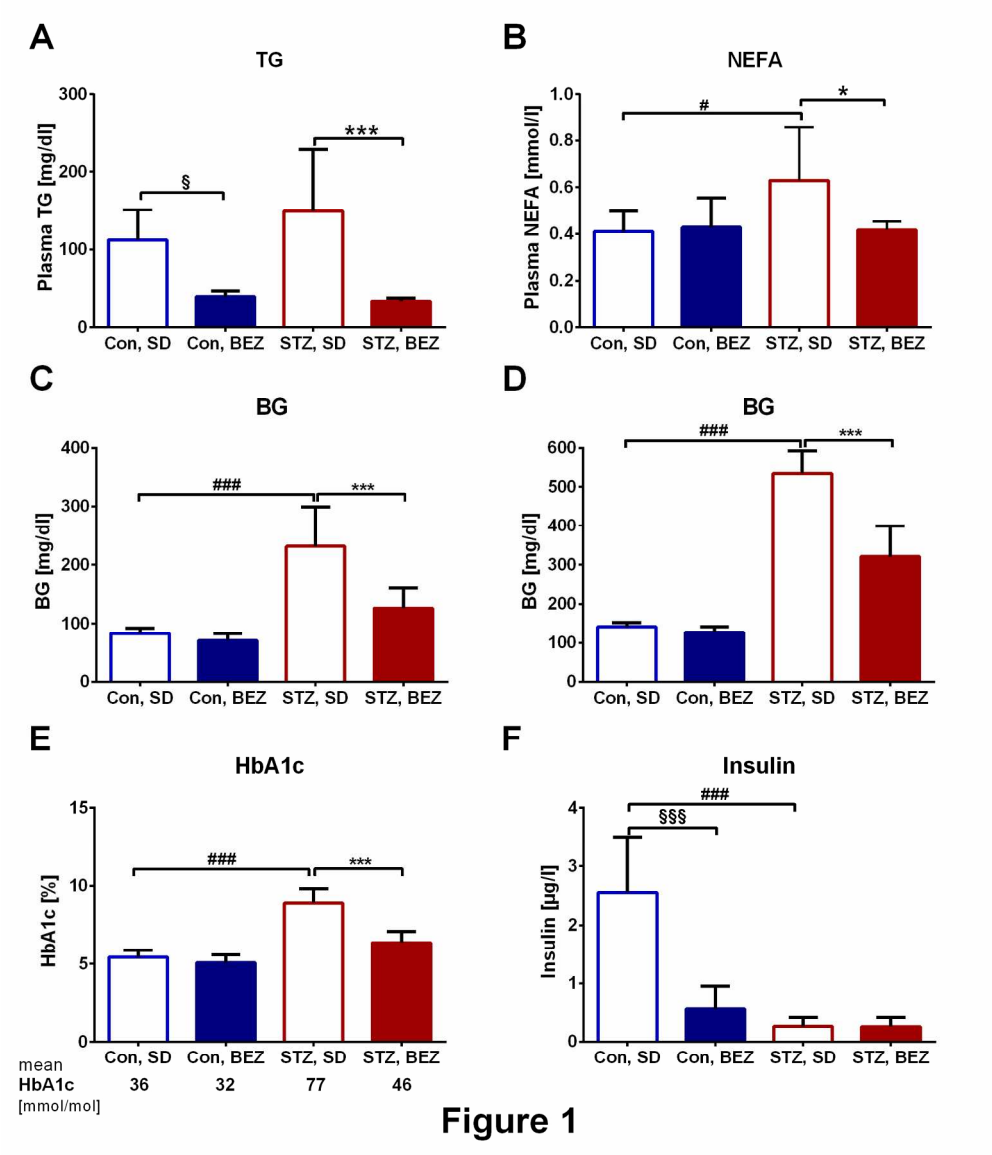

Figure 1

Fig. 1 Levels of plasma lipid, insulin, blood glucose and HbA1c in STZ mice
180x208mm (300 x 300 DPI)

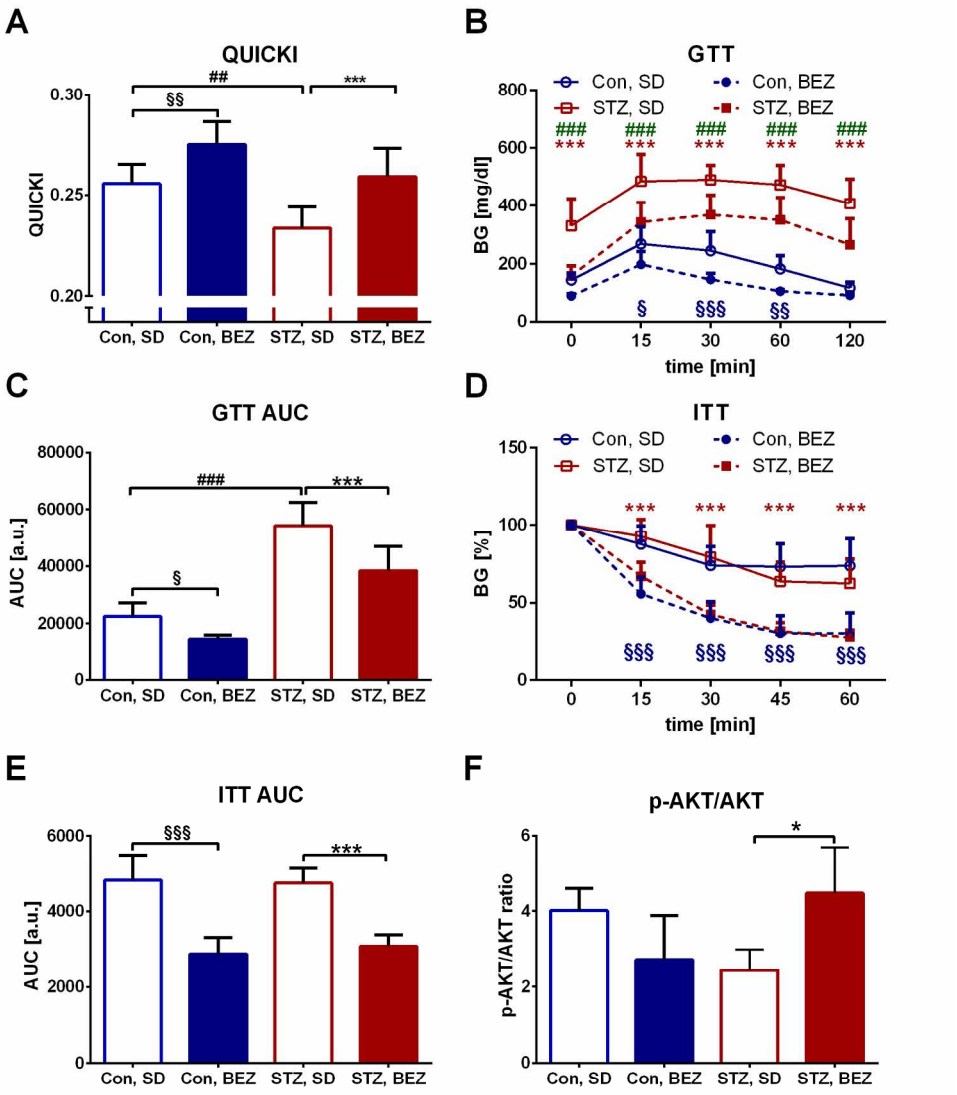

Figure 2

Fig. 2 QUICKI, glucose-, insulin-tolerance tests and muscle p-AKT/AKT ratio in STZ mice
180x220mm (300 x 300 DPI)

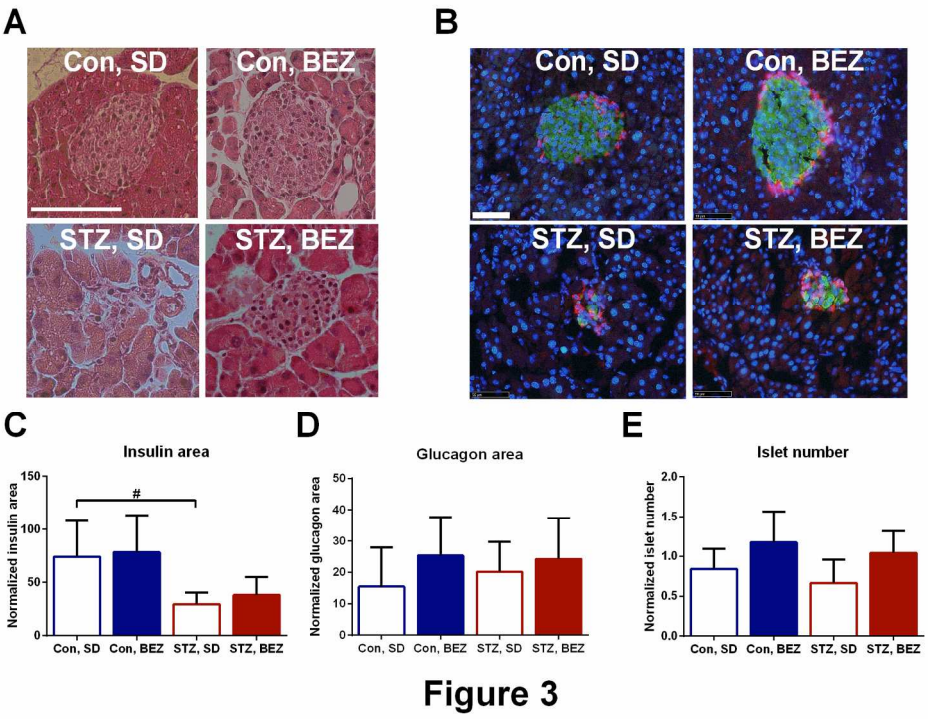

Figure 3

Fig. 3 Pancreas architecture in STZ mice
180x134mm (300 x 300 DPI)

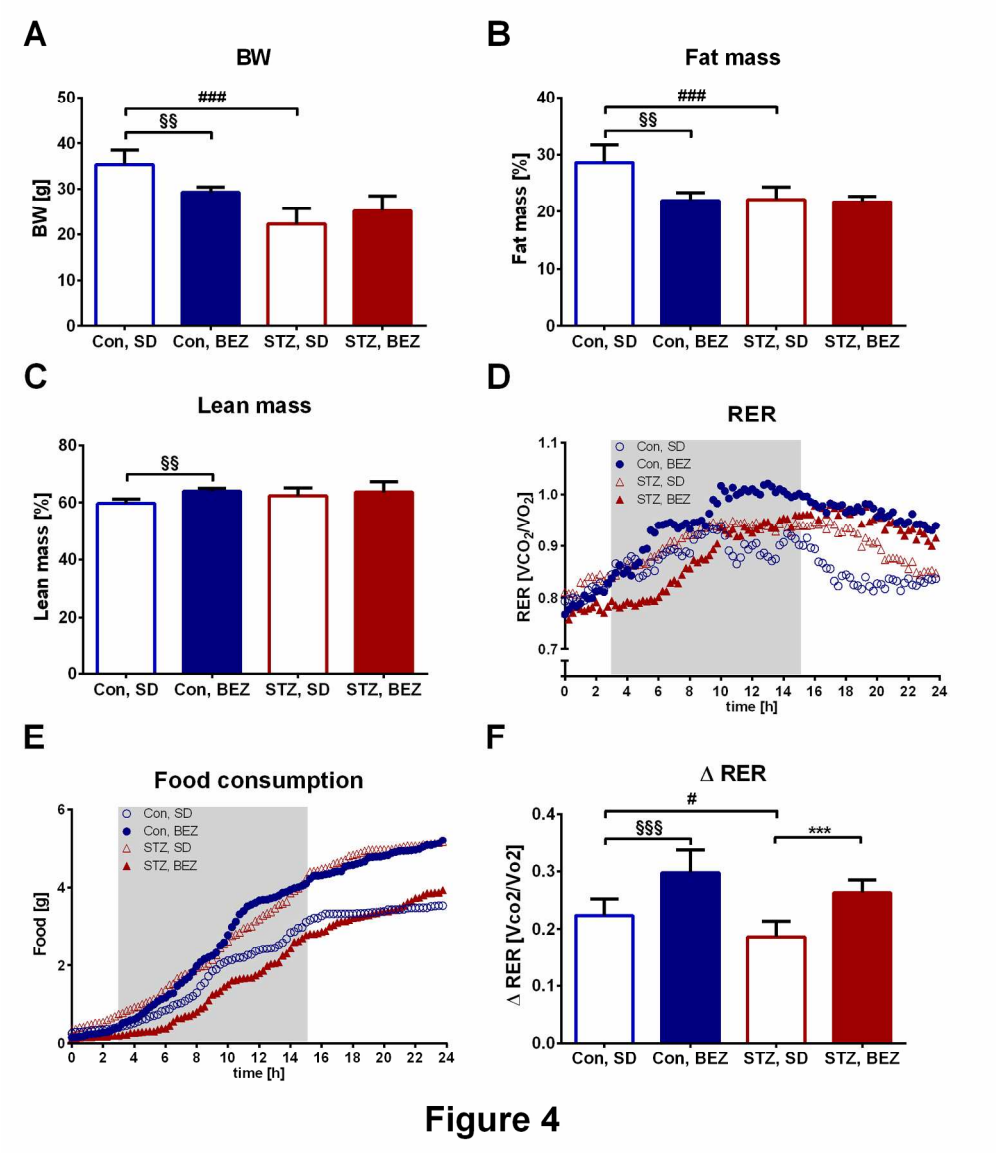

Figure 4

Fig. 4 Body composition and indirect calorimetry in STZ mice
180x208mm (300 x 300 DPI)

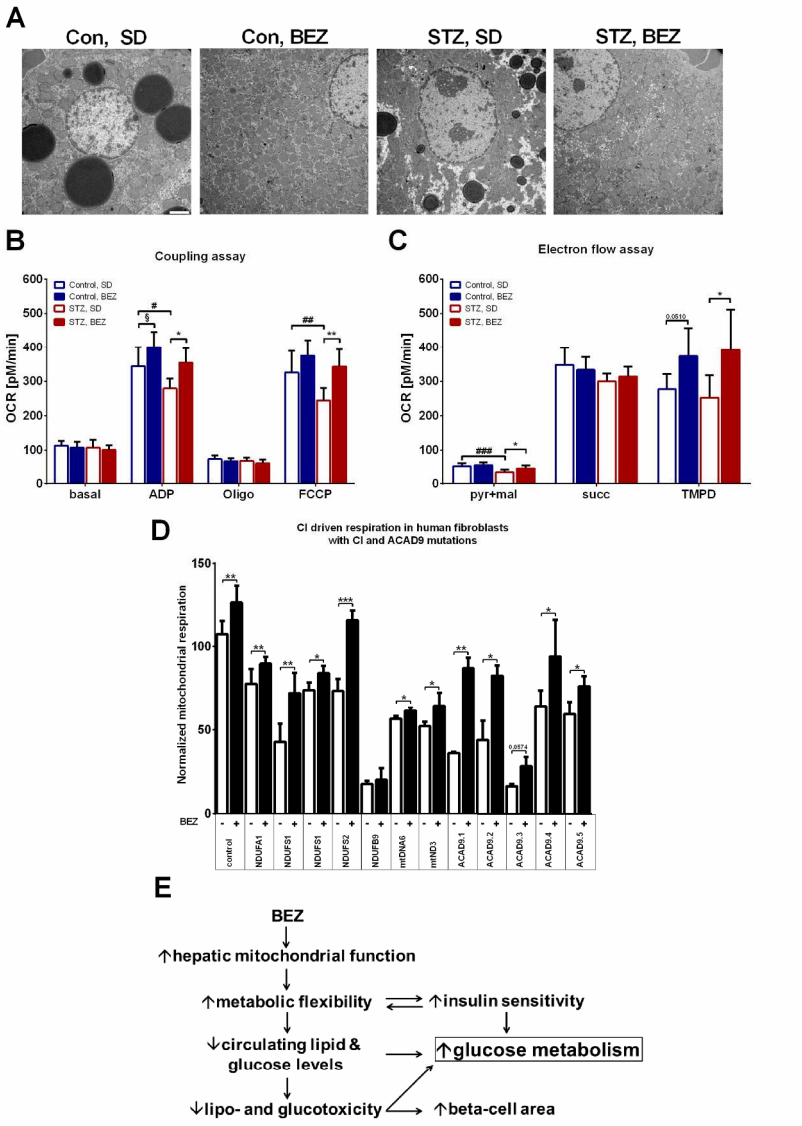

Figure 5

Fig. 5 Mitochondrial mass in STZ mouse livers and mitochondrial function in BEZ-treated STZ mice and human fibroblasts
180x264mm (300 x 300 DPI)

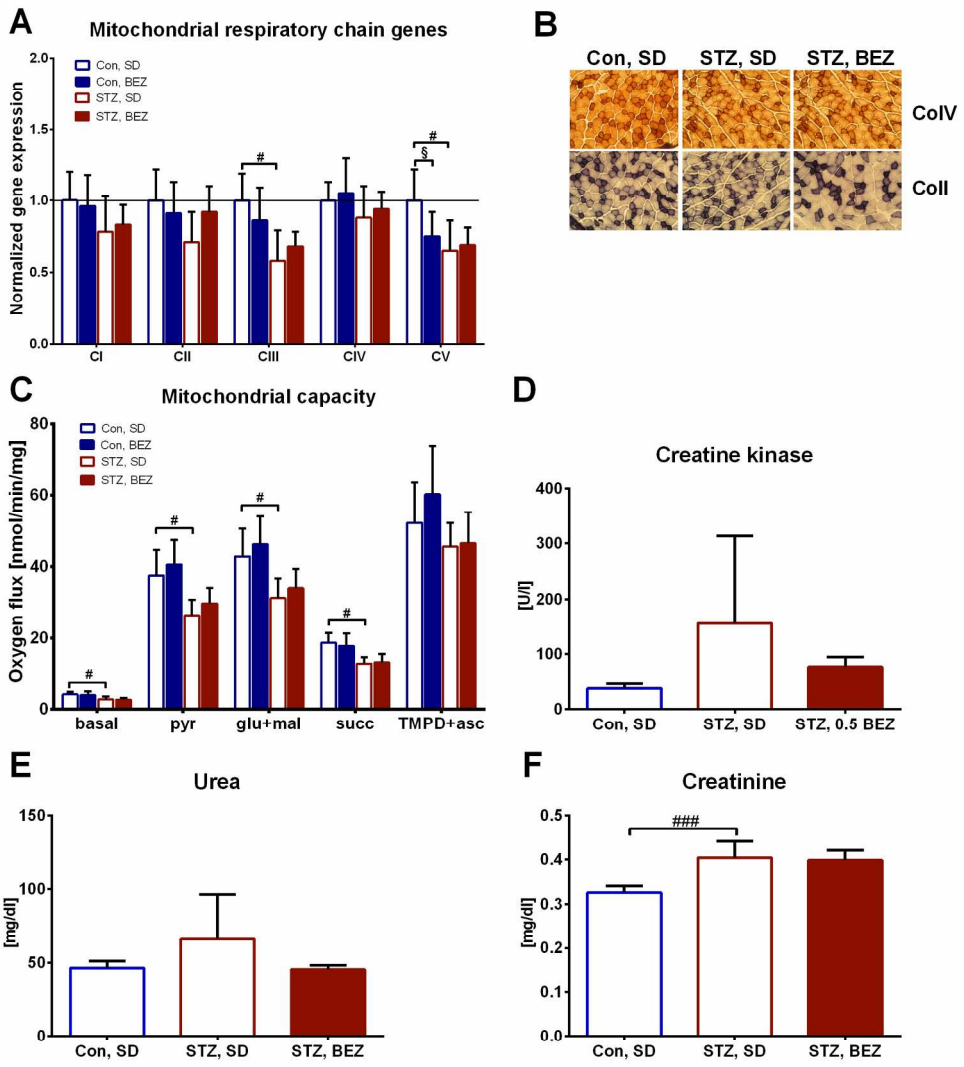

Suppl. Figure 1

180x208mm (300 x 300 DPI)

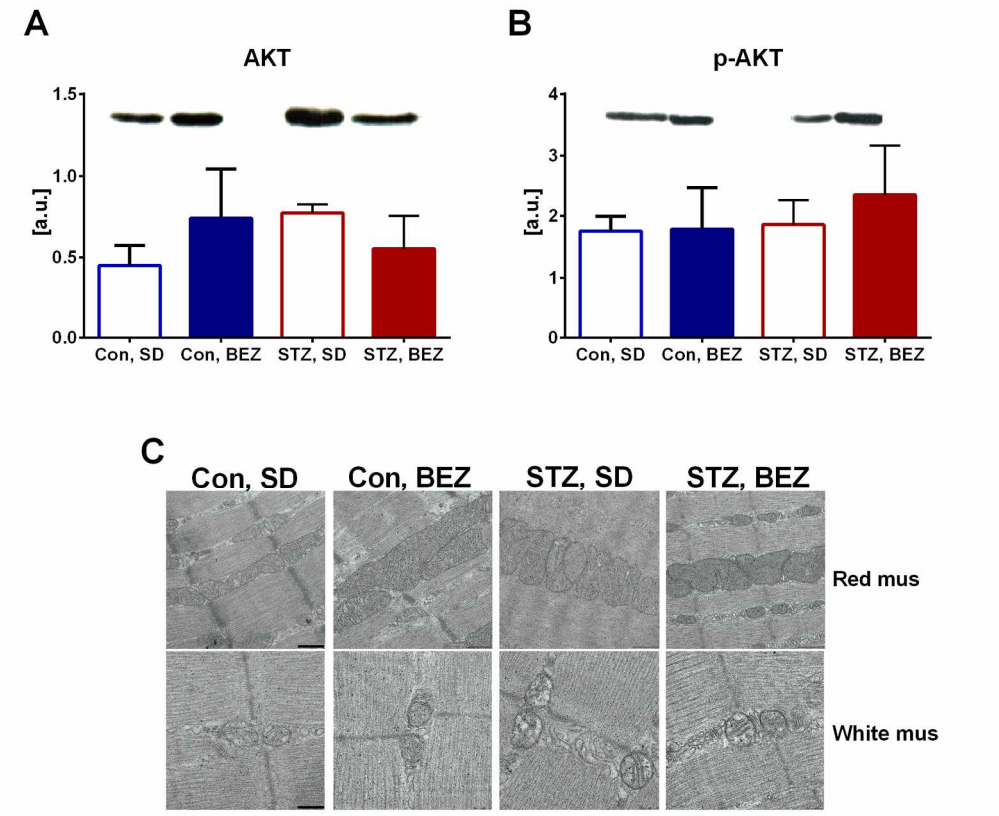

Suppl. Figure 2

180x162mm (300 x 300 DPI)

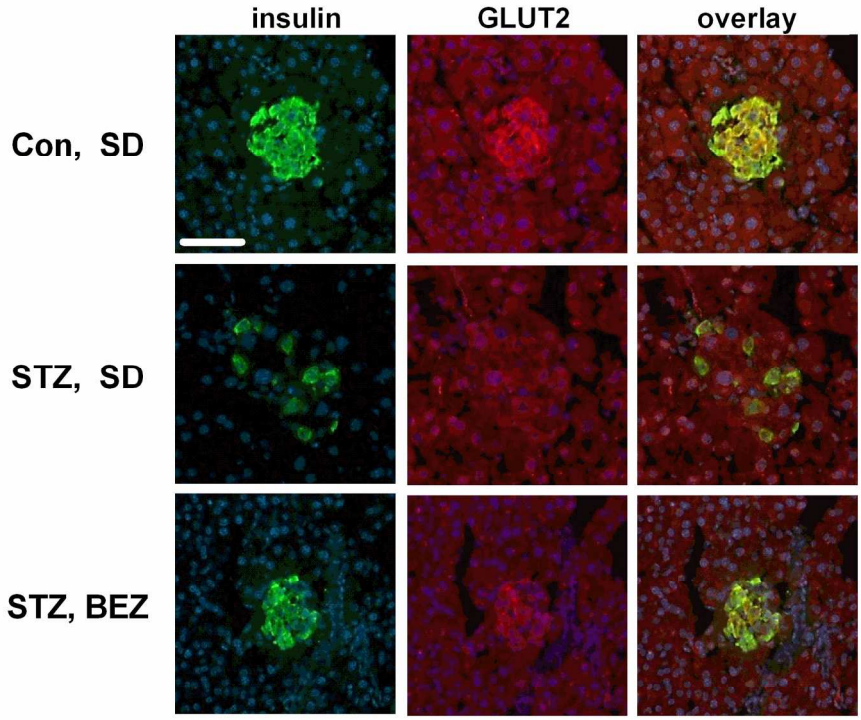

Suppl. Figure 3

180x152mm (300 x 300 DPI)

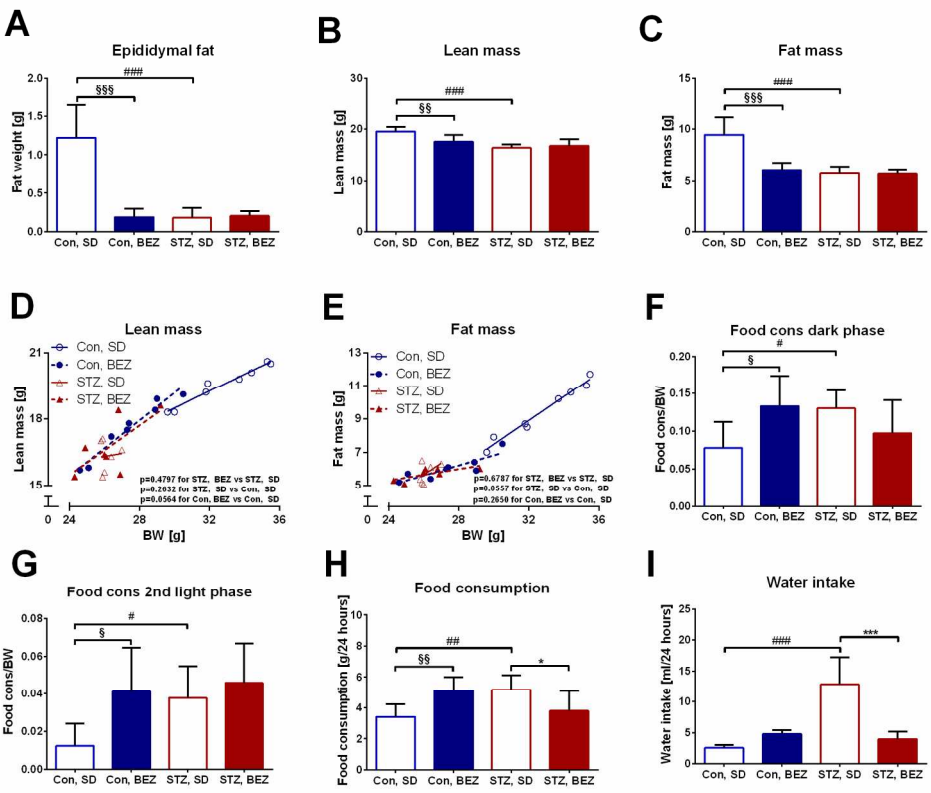

Suppl. Figure 4

180x163mm (300 x 300 DPI)

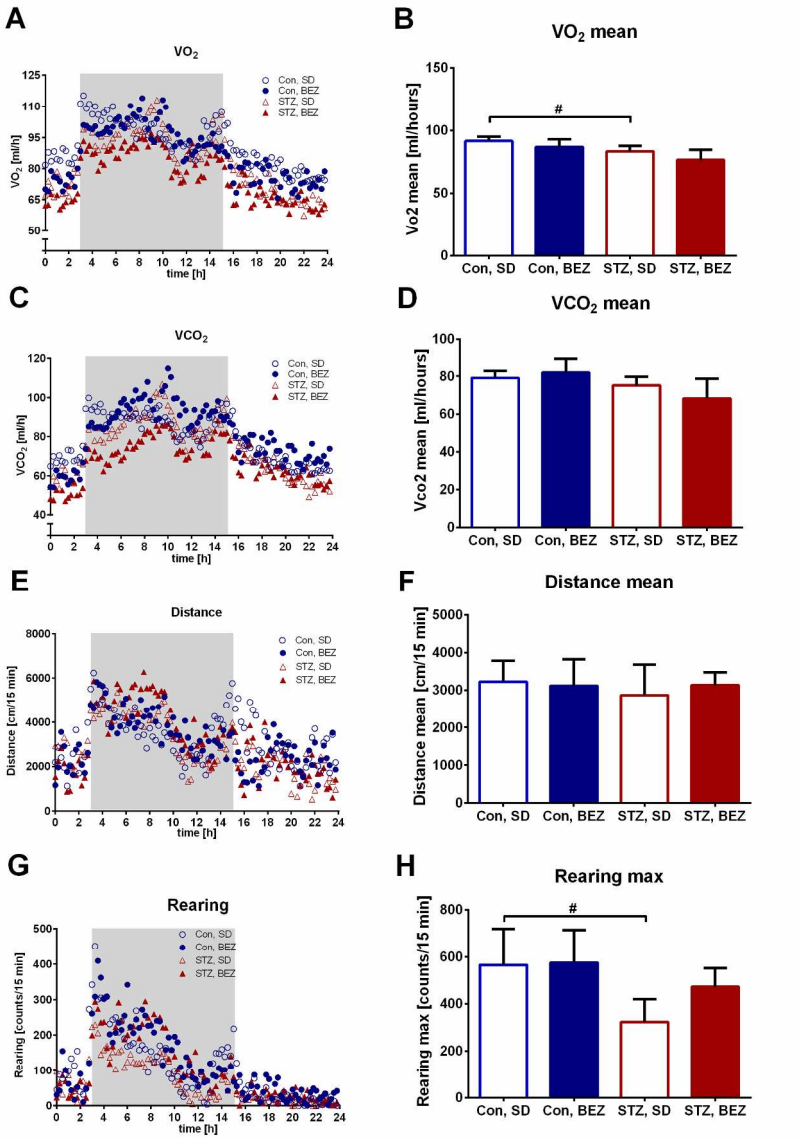

Suppl. Figure 5

180x262mm (300 x 300 DPI)

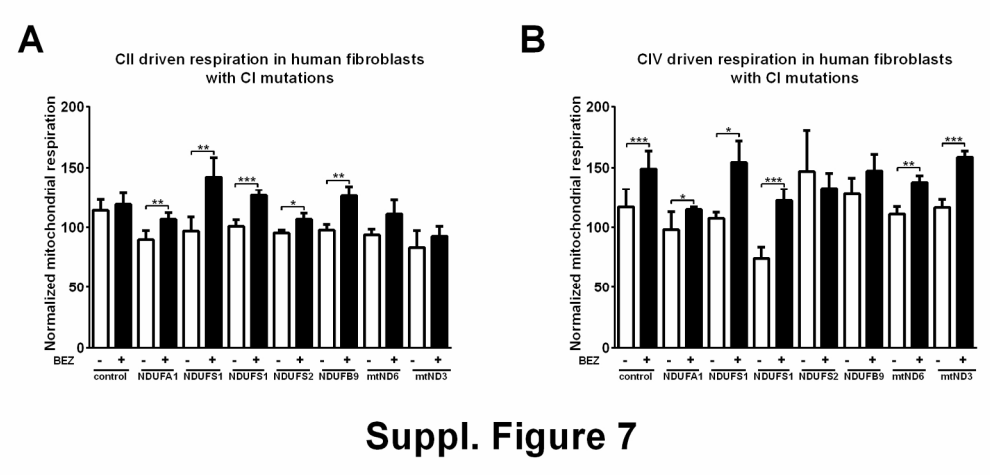

Suppl. Figure 7

180x86mm (300 x 300 DPI)

Supplementary figure legends and tables

Suppl. Fig. 1 Mitochondrial function in skeletal muscle and plasma parameters of STZ mice

A Expression of representative subunits of the mitochondrial respiratory chain was analyzed by real time PCR in *tibialis cranialis* muscle. C denotes mitochondrial complexes I-V. Gene expression was normalized to housekeeping gene and Con, SD group. **B** Histochemical staining representing Complex IV (CoIV, brown staining, upper panels) and Complex II (CoII, blue staining, lower panels) activities in situ, images were acquired by 200x magnifications in *gastrocnemius* muscle. Representative areas are shown. **C** Oxygen consumption in saponin skinned *soleus* fibers was measured by high-resolution respirometry (Oroboros) with the denoted substrates added to the chambers. basal:pyruvate was used in the absence of ADP; pyr:ADP; glu:glutamate; mal:malate; succ:succinate; TMPD: tetramethylphenylendiamin; asc:ascorbate. A, C represent n=4-8 animals, while B represents n=3 animals. **D-F** Plasma parameters measured by clinical chemistry. **#** denotes significant differences between STZ, SD vs. Con, SD; #p<0.05; ###p<0.001, **§** denotes significant differences between Con, BEZ vs. Con, SD; §p<0.05,

Suppl. Fig. 2 Phospho-AKT levels and mitochondrial mass in skeletal muscle of STZ mice

A anti-AKT and **B** anti-phospho-473-AKT antibodies were used in Western blot to visualize protein levels from *quadriceps* muscles. **C** Mitochondrial morphology and mass was assessed by transmission EM from *quadriceps* muscles. Upper panels represent red, lower panels represent white muscle fibers at 10.000x and 20.000x magnification, respectively. Black bars denote 500 nm in the upper and 200 nm in the lower panels, respectively. Representative areas are shown. Columns represent averages+standard deviations; n=4-5 animals.

Suppl. Fig. 3 Insulin and GLUT2 staining in pancreata of STZ mice

Pancreata were stained with anti-insulin (green) and anti-GLUT2 (red) antibodies and visualized by fluorescent microscopy. Cell nuclei were stained with DAPI (blue). White bar represents 50 μm. Representative areas are shown from n=3 animals.

Suppl. Fig. 4 Body composition and indirect calorimetry in STZ mice

A Epididymal fat weight. **B** Lean and **C** fat mass were measured by qNMR and these values were **D-E** normalized to body weight. **F** Food consumption in the dark and **G** second light phase. **H** Food consumption and **I** water intake. Columns represent averages+standard deviations; n=6-8 animals. For calculating p-values ANOVA and Holm-Sidak´s tests were applied for A-C and F-I. For D-E linear regression analysis were applied and calculated p-values are indicated in the figures. ***** denotes significant differences between STZ, BEZ vs. STZ, SD; *p<0.05, ***p<0.001; **#** denotes significant differences between STZ, SD vs. Con, SD; #p<0.05, ##p<0.01, ###p<0.001; **§** denotes significant differences between Con, BEZ vs. Con, SD; §p<0.05, §§p<0.01, §§§p<0.001.

Suppl. Fig. 5 Indirect calorimetry in STZ mice

A Oxygen consumption (VO_2), **C** carbon dioxide production (VCO_2), **E** run distance and **G** rearing were measured and appropriate mean as well as maximum values were calculated **B, D, F, H**. Gray rectangle represents 12 hours dark phase (0 time point represents 3 p.m.). Columns represent averages+standard deviations; n=7-8 animals. **#** denotes significant differences between STZ, SD vs. Con, SD; #p<0.05.

Suppl. Fig. 6 Hepatic gene expression in STZ mice

Hepatic gene expression was studied by real-time PCR. Gene expression data were normalized to Con, SD, denoted at 1 with dashed line. Gene names are given in Suppl. Table 1. **A** Genes for inflammatory pathways. **B** Target genes for PPAR and insulin pathway. The possible upstream regulators were taken from Ingenuity database and are denoted under the graphic. **C** Mitochondrial genes. Columns represent averages+standard deviations; n=5-7

animals. * denotes significant differences between STZ, BEZ vs. STZ, SD; *p<0.05, **p<0.01, ***p<0.001; # denotes significant differences between STZ, SD vs. Con, SD; #p<0.05, ##p<0.01, ###p<0.001.

Suppl. Fig. 7 Mitochondrial function in human fibroblasts treated with BEZ

Mitochondrial respiration was determined using high resolution respirometry and **A** succinate as complex II substrate or **B** TMPD as complex IV substrates; subsequently potassium cyanide was applied the loci of the mutation for the appropriate subunits of complex I are indicated under the figure. Data are normalized to the lowest value of untreated control samples. For control fibroblasts n=7-33, for patients fibroblasts n=3-11 replicates were performed and students t-tests were used for calculating p-values. * denotes significant differences between BEZ treated and untreated fibroblasts; *p<0.05, **p<0.01, ***p<0.001.

Suppl. Table 1 Primer sequences used for liver real-time PCR

Symbol	Gene	Entrez	5´primer	Tm	3´primer	Tm	Length
Acaa1b	acetyl-Coenzyme A acyltransferase 1B	235674	CTGCTTCAAGGACACCACCC	60.89	GAGATGTCTCCCAGCTGCTC	59.9	99
Acaca	acetyl-Coenzyme A carboxylase alpha	107476	ACACCTGAAGACCTTAAAGCCA	59.56	CCAGCCCACACTGCTTGTA	59.93	152
Atp9a	ATPase, class II, type 9A	11981	CCTCCCTCTGCCACTCAAAG	60.04	ACAGCACCTGGGCTGACATT	62.07	82
Cidec	cell death-inducing DFFA-like effector c	14311	AAGCGCATCGTGAAGGAGAT	59.82	CATGTAGCTGGAGGTGCCAA	60.04	87
Cox19	COX19 cytochrome c oxidase assembly homolog (S. cerevisiae)	68033	GTCGACCGCAATGAACTTCG	59.91	ACATTCACCGAAGTGGTCCAG	60.27	88
Csad	cysteine sulfinic acid decarboxylase	246277	CTGCTCCCTCTGCTTCTGTC	60.11	GGATGAAATCTTCCAGCTCAGG	58.79	109
Cyp2b10	cytochrome P450, family 2, subfamily b, polypeptide 10	13088	GCTTTGAGTACACAGACCGTCA	60.55	AGAGAAGAGCTCAAACATCTGG	57.79	104
Fabp2	fatty acid binding protein 2, intestinal	14079	GGACTGGACCTCTGCTTTCC	60.04	TCTACTTTCCACGTGCCGTC	60.04	72
Fabp5	fatty acid binding protein 5, epidermal /// fatty acid binding protein 5-like 2	16592	CATGGCCAAGCCAGACTGTA	60.04	GGTGCAGACCGTCTCAGTTT	60.25	154
Gadd45g	growth arrest and DNA-damage-inducible 45 gamma	23882	AGTCCTGAATGTGGACCCTG	59.01	GCAGAACGCCTGAATCAACG	60.18	112
Gck	glucokinase	103988	TTGCAACACTCAGCCAGACA	60.11	TGCTCTACCAGAGTCAACGAC	59.46	147
Ifit1	interferon-induced protein with tetratricopeptide repeats 1	15957	TCTGCTCTGCTGAAAACCCA	59.53	CACCATCAGCATTCTCTCCCAT	60.16	70
Ly6c2	lymphocyte antigen 6 complex, locus C2 /// lymphocyte antigen 6 complex, locus C1	100041546	ACGCTACAAAGTCCTGTTTGC	59.4	CTGCAGTCCCTGAGCTCTTC	60.11	71
Ndufab1	NADH dehydrogenase (ubiquinone) 1, alpha/beta subcomplex, 1	70316	CACCCCCACTGACGTTAGAC	60.04	ACGGAGAGCTTTTCTGGATCA	59.1	88
Pck1	phosphoenolpyruvate carboxykinase 1, cytosolic	18534	ATGAAAGGCCGCACCATGTA	60.03	GGGCGAGTCTGTCAGTTCAA	59.97	93
Pdk4	pyruvate dehydrogenase kinase, isoenzyme 4	27273	TTTCCAGGCCAACCAATCCA	59.81	GGCCCTCATGGCATTCTTGA	60.4	87
Scarb1	scavenger receptor class B, member 1	20778	TGATGCCCCAGGTTCTTCAC	59.96	TGTCTTCAGGACCCTGGCT	60.15	108
Scd1	stearoyl-Coenzyme A desaturase 1	20249	CAGGTTTCCAAGCGCAGTTC	60.04	ACTGGAGATCTCTTGGAGCA	57.76	142
Stat3	signal transducer and activator of transcription 3	20848	GTGTGACACCATTCATTGATGC	58.5	TCCTCACATGGGGGAGGTAG	60.03	132
Tifa	TRAF-interacting protein with forkhead-associated domain	211550	AAGTCCCCAGGAGAGGAGACAA	62.19	GGCCAGGATGGTAAATGGTCA	60.06	153

Symbol	Gene	Entrez	Qiagen Assay name	Qiagen Cat. No.
Cpt1b	carnitine palmitoyltransferase 1b, muscle	12895	Mm_Cpt1b_1_SG	QT00172564
Cpt2	carnitine palmitoyltransferase 2	12896	Mm_CPT2_1_SG	QT00304717

Suppl. Table 2 Blood parameters in random fed mice

	Con, SD	Con, 0.25% BEZ	Con, 0.5% BEZ	STZ, SD	STZ, 0.25% BEZ	STZ, 0.5% BEZ
TG [mg/dl]	**112.2**±38.6	**29.86**±5.9§§§	**40.11**±7.1§§	**149.1**±79.3	**29.93**±3.7***	**34.2**±3.8***
NEFA [mmol/l]	**0.41**±0.09	**0.35**±0.08	**0.43**±0.13	**0.63**±0.23#	**0.42**±0.07*	**0.42**±0.04*
BG [mg/dl]	**147.7**±11.1	**144.9**±13.5	**127.9**±13.8	**534.7**±58.1###	**399.0**±87.3***	**320.4**±78.8***

Triglyceride (TG) and non-esterified fatty acids (NEFA) were measured by routine clinical chemistry data from plasma and blood glucose (BG) from tail blood. Numbers represent averages±standard deviations; n=4-7 animals. ***** denotes significant differences between STZ, BEZ vs. STZ, SD; *p<0.05, ***p<0.001; **#** denotes significant differences between STZ, SD vs. Con, SD; #p<0.05, ###p<0.001; **§** denotes significant differences between Con, BEZ vs. Con, SD; §§p<0.01, §§§p<0.001.

Suppl. Table 3 Expression of hepatic genes involved in fatty acid oxidation normalized to STZ, SD group and depicted as fold changes

Gene symbol	Gene name	STZ, BEZ/ STZ, SD
ACAA1b	acetyl-Coenzyme A acyltransferase 1B	**4.87**
ACAA2	acetyl-Coenzyme A acyltransferase 2 (mitochondrial 3-oxoacyl-Coenzyme A thiolase)	**1.22**
ACADL	acyl-Coenzyme A dehydrogenase, long-chain	**1.89**
ACADM	acyl-Coenzyme A dehydrogenase, medium chain	**1.68**
ACADS	acyl-Coenzyme A dehydrogenase, short chain	**1.39**
CPT1B	carnitine palmitoyltransferase 1b, muscle /// cDNA sequence BC090627	**14.51**
CPT2	carnitine palmitoyltransferase 2	**1.92**
EHHADH	enoyl-Coenzyme A, hydratase/3-hydroxyacyl Coenzyme A dehydrogenase	**3.48**
FABP1	fatty acid binding protein 1, liver	**2.68**
FABP2	fatty acid binding protein 2, intestinal	**3.28**
FABP3	fatty acid binding protein 3, muscle and heart	**28.82**
FABP4	fatty acid binding protein 4, adipocyte	**3.20**
HADHA	hydroxyacyl-Coenzyme A dehydrogenase (trifunctional protein), alpha subunit	**1.74**
HADHB	hydroxyacyl-Coenzyme A dehydrogenase (trifunctional protein), beta subunit	**2.26**

Genes involved in fatty acid oxidation were selected from liver microarray data, comparing BEZ treated STZ mice to STZ, SD controls. Array data has been submitted to the GEO database at NCBI (GSE39752, GSE79008).

Suppl. Table 4 Fold changes of plasma metabolite levels (33 out of 52), which show inverse regulation between STZ, BEZ vs STZ, SD and STZ, SD vs Con, SD comparisons

Metabolites	STZ, SD/Con, SD	STZ, BEZ/STZ, SD	
Creatinine	-1.1	1.2	
Putrescine	-1.5	2.2	
Trp	-1.5	1.5	
Orn/Arg	-1.3	2.2	
PC aa C30:0	-1.6	1.5	
PC aa C32:0	-1.7	1.7	
PC aa C32:1	-10.1	9.0	
PC aa C32:2	-2.7	2.4	
PC aa C34:1	-3.6	4.0	
PC aa C34:3	-1.5	1.9	
PC aa C36:1	-2.2	1.9	
PC aa C36:3	-1.7	2.4	
PC aa C38:3	-2.1	2.1	
PC aa C38:5	-1.5	1.6	
PC aa C40:3	-3.7	2.1	
PC aa C40:4	-2.2	1.9	
PC ae C32:1	-1.9	2.2	
PC ae C34:1	-2.2	2.3	
PC ae C34:2	1.8	-2.2	
PC ae C36:2	2.1	-2.2	
PC ae C38:4	2.0	-2.1	
PC ae C40:3	-1.5	1.6	
PC ae C40:6	1.7	-3.2	
PC ae C42:0	-2.4	1.7	
PC ae C42:4	1.6	-2.3	*
SM (OH) C16:1	1.8	-1.8	
SM C20:2	-1.4	1.8	
SM C24:1	-1.6	2.7	
PUFA (PC) / MUFA (PC)	3.8	-4.1	*
PUFA (PC) / SFA (PC)	1.5	-1.3	*
PUFA (LPC) / MUFA (LPC)	3.9	-4.4	*
Total AC / C0	1.6	-1.5	*
Total SM-OH / Total SM-non OH	1.4	-1.5	*

STZ treatment significantly altered the level of 85 metabolites and metabolite ratios compared to Con, SD animals (left column). On the other hand, BEZ treatment of STZ mice significantly altered 78 metabolites and metabolite ratios compared to STZ, SD mice (right

column). Among these comparisons there were 54 common metabolites and metabolite ratios, 52 of them showed inverse regulation. Numbers denote fold changes calculated by dividing the appropriate means of groups. The original data are shown as Suppl. Table 5.

AC:acylcarnitine, numbers after PC or SM denote the length of carbon chain, the numbers after : denote the number of double bounds, LPC:lysophosphatidyl choline, MUFA:monounsaturated fatty acid, SFA:saturated fatty acid, PUFA:polyunsaturated fatty acid, PC:phosphatidyl choline, SM:sphingomyelin, C0: free carnitine, aa:acyl-acyl, ae:acyl-ether. * denotes values, which were lower than 3-times zero values.